Food Chemistry 172 (2015) 335–342

Contents lists available at ScienceDirect

Food Chemistry

journal homepage: www.elsevier.com/locate/foodchem

Analytical Methods

Multilayer graphene–gold nanocomposite modified stem-loop DNA biosensor for peanut allergen-Ara h1 detection

Xiulan Sun [a,*], Min Jia [a], Lu Guan [a], Jian Ji [a], Yinzhi Zhang [a], Lili Tang [a], Zaijun Li [b]

[a] State Key Laboratory of Food Science and Technology, School of Food Science and Technology, Synergetic Innovation Center of Food Safety and Nutrition, Jiangnan University, Wuxi, Jiangsu 214122, China
[b] School of Chemical and Material Engineering of Jiangnan University, Wuxi, Jiangsu 214122, China

ARTICLE INFO

Article history:
Received 11 October 2013
Received in revised form 20 June 2014
Accepted 10 September 2014
Available online 17 September 2014

Keywords:
Electrochemical biosensor
Stem-loop probe
Graphene–gold nanocomposite
Peanut allergen
Arachis hypogaea allergen 1 (Ara h1)

ABSTRACT

In this study, we developed an electrochemically-amplified, stem-loop DNA biosensor to detect the peanut allergen Ara h1. Specifically, we electrodeposited a multilayer graphene–gold nanocomposite onto a glassy carbon electrode and then immobilised a thiolated hairpin DNA–biotin probe onto the modified electrode surface. The multilayer graphene–gold composite has good dispersion ability, and can amplify the electrochemical signal due to its high electron-transfer efficiency. The probe was switched to an "off" state in the presence of target DNA. The prepared biosensor demonstrated a linear response ranging from 10^{-16} to 10^{-13} M, with an ultrasensitive detection limit of 0.041 fM. Moreover, the biosensor showed excellent selectivity, as well as the ability to discriminate between a complementary target and a one-base mismatch or non-complementary sequence. Results show that this prepared DNA biosensor can be successfully used to detect the peanut allergen Ara h1 in a peanut milk beverage. Findings can be applied to the prevention of allergic reactions, thus improving human health and safety.

1. Introduction

As scientific research moves into the era of genomics, sequence-specific DNA detection has attracted attention due to its wide-ranging applications, including virus detection (Daming Huang, Zhang, Jiao, & Xun, 2009), diagnosis of genetic diseases (Yin, Zhou, Zhang, Meng, & Ai, 2012) and prevention of bioterrorism (Espy et al., 2002). The development of instruments and methods for accurate sequence-specific DNA analysis is essential for the efficient use of genomic information. To this end, various techniques have been developed for DNA detection, such as chromosome analysis (Zuccarelli et al., 2011), fluorescence in situ hybridization (Barr Fritcher et al., 2008) and real-time, quantitative reverse-transcription polymerase chain reaction (PCR) (Mekata et al., 2009). However, these techniques have several limitations, including the time required, low accuracy and high cost. Therefore, development of a rapid and effective method for DNA detection is timely and necessary.

Electrochemical DNA biosensors are now commonly used for specific gene detection due to unique advantages, such as low cost, simplicity, good selectivity and high sensitivity (Wang, Zhang, & Zhang, 2010). These sensors can be prepared by immobilising single-stranded DNA probes onto an electrode surface and using electroactive indicators (Lin et al., 2009) or other methods (Chen, Zhang, Yang, Fu, & Chen, 2010; Fan et al., 2010) to measure hybridization events between DNA probes and their complementary DNA fragments. Of the various probes used for nucleic acid detection, stem-loop structured DNA probes are superior to linear probes for several reasons (Bockisch, Thomas, Edzard, & Reinhard, 2005). Their largest draw is their superior ability to distinguish even single-base mismatches from the complementary target sequence (Summerer & Marx, 2002). Stem-loop structured DNA probes also show great potential for real-time monitoring. Some researchers refer to the stem-loop probe as a "molecular beacon" (Goel, Kumar, Puniya, Chen, & Singh, 2005). This single-stranded, nucleic acid probe forms a hairpin-like secondary structure in the absence of its target strand. The actual probe sequence is situated in the loop part of the strand, and the stem is formed by base-pairing the two complementary arm sequences at either side of the loop.

In recent years, a variety of stem-loop probe electrochemical sensors have been developed (Ehsan Salamifar & Lai, 2014; Yu & Lai, 2012). For example, Rai et al. (2012) constructed an electrochemically-amplified molecular beacon biosensor using thiolated hairpin DNA–ferrocene probes on a gold electrode for ultrasensitive DNA sequence-specific detection of *Legionella* species. This biosensor demonstrated a linear range over 8 orders of magnitude with an ultrasensitive detection limit of 2.3×10^{-14} M for the

* Corresponding author. Tel./fax: +86 510 85328726.
E-mail address: sxlzzz@jiangnan.edu.cn (X. Sun).

http://dx.doi.org/10.1016/j.foodchem.2014.09.042
0308-8146/

quantification of a 21-mer DNA sequence. Kjallman et al. (2010) reported a CdTe nanoparticle-modified hairpin probe for direct, sensitive electrochemical detection of DNA. Impedance spectroscopy has also been used to examine the electron transfer processes in a modified gold electrode before and after hybridization with target DNA. The sensor showed reliable, sensitive detection of 4.7 fM for the target. Lin et al. (2011) developed an enzyme-amplified electrochemical biosensor to detect the PML-RAPα fusion gene, based on a hairpin locked nucleic acid probe. This was dually labelled with biotin and a carboxyfluorescein molecule (FAM). The probe was immobilised at a streptavidin-modified electrode surface via the biotin-streptavidin bridge, where the FAM group served as an affinity tag for peroxidase conjugate binding. This new biosensor demonstrated an excellent specificity for single-base mismatching and an ability to detect as little as 83 fM of the target DNA, even in the presence of human serum. Liu et al. (2011) reported an ultrasensitive signal-on DNA biosensor, based on a endonuclease-assisted electrochemistry signal amplification. They used a 5′-thiol, modified, hairpin-shaped probe (HP) and a 3′-ferrocene (Fc)-labelled probe (Fc-PCP). When the HP was hybridized with the target DNA to form a duplex, the endonuclease was added and observed to nick the HP strand in the duplex. Next, an Fc-PCP was introduced to hybridize with the residual HP fragment, resulting in generation of the electrochemical signal. The present DNA biosensor showed a low detection limit of 0.167 pM to detect the target DNA.

In the aforementioned studies, all electrode surfaces of the fabricated DNA biosensors were not modified. If the electrode surface can be modified with nanometre materials, the electrochemical signal will be amplified, and the detection limit of the sensor will increase further. In recent years, nanomaterials have been widely used in electrode surface modification due to their high surface area, favourable electronic properties and electrocatalytic activity, as well as good biocompatibility related to nanometre size (Guo, Wen, Zhai, Dong, & Wang, 2010; Pumera, Sanchez, Ichinose, & Tang, 2007). Graphene and gold nanoparticles are ideal nanomaterials for development of electrochemical sensors due to their simple preparation, relatively low cost and huge molecular interfaces. Graphene is a monolayer of carbon atoms that tightly stacks to form a hexagonal, honeycomb-like lattice crystal structure (Li et al., 2009). Owing to its unique two-dimensional structure, graphene exhibits some excellent properties, such as a large specific surface area, high thermal and electrical conductivity, and mechanical strength (Elias et al., 2009; Yan, Cui, & Li, 2010). However, large Van der Waals forces between graphene sheets make them easy to accumulate and aggregate. This limits graphene's application in many fields. One solution is inserting noble metal nanoparticles between graphene sheets to form an electrocatalysis system (Xu, Wang, & Zhu, 2008; Zhong et al., 2010). This method can prevent aggregation of graphene sheets and greatly improve electron conductivity between the sheets.

Gold nanoparticles (AuNPs) have good conductivity, biocompatibility and electrocatalytic activity of the corresponding sensor. Recently, graphene/gold composite materials have been used in biosensors. Hong et al. (Wenjing Hong, Yuxi, Yao, Zhongze, & Shi, 2010) reported the self-assembly of positively-charged AuNPs on negatively-charged 1-pyrene butyric acid functionalized graphene (PEG) sheets. The AuNP–PEG composite was modified on the glassy carbon electrode (GCE) surface to form a uric acid electrochemical sensor with rapid-response capability and high sensitivity. Gu et al. (2011) developed an ultrasensitive electrochemical biosensor for glucose using CdTe–CdS core–shell quantum dots to establish an ultrafast electron transfer relay between the graphene–gold nanocomposite and the AuNPs. The biosensor showed high sensitivity, a low detection limit, a fast response time, a wide calibration range, and good long-term stability. With its many benefits in terms of reproducible, simple, and rapid, the one-step electrochemical deposition technique is now one of the most useful methods for preparation of AuNPsn (Paunovic, 2007; Zheng, Zhang, Li, & Shen, 2002). In our study, a multilayer graphene–gold nanocomposite was obtained by simple, direct electrochemical deposition, which can greatly amplify the electrochemical signal and further increase the detection limit of the sensor (0.041 fM).

Herein, we prepared a stem-loop DNA probe biosensor using a multilayer graphene–gold nanocomposite as a signal amplification material. We adopted a cycle-alternate electrodeposition method to deposit monolayers of graphene and AuNPs on the electrode surface to form a multilayer graphene–gold nanocomposite. A compact gold film was then electrodeposited on top of the multilayer composite to form the anchoring site to immobilize the probe. We used a stem-loop probe, dually labelled with 5′-SH and 3′-biotin, to self-assemble on the gold film surface with facile Au–S affinity. The purpose of this study was to prepare a multilayer graphene–gold nanocomposite, design an appropriate stem-loop probe, evaluate the sensitivity and selectivity of the electrochemical DNA sensor, and detect target samples with this biosensor.

2. Experimental

2.1. Materials and apparatus

All synthetic oligonucleotides were purchased from Sangon Biotech Co., Ltd. (Shanghai, China). The sequences of oligonucleotides used in this work are given in Table 1. 6-Mercaptohexanol (MCH) was obtained from Sigma–Aldrich. Graphene oxide was synthesized from natural flake grapheme by the Hummers method (Park & Ruoff, 2009). All other chemicals were obtained from Sinopharm Chemical Reagent Co., Ltd. The 0.1 mg mL^{-1} graphene oxide suspension was prepared by suspending graphene oxide in phosphate buffer (0.1 M, pH 7.0). The 0.1 mM $HAuCl_4$ solution was prepared by dissolving in 0.5 M H_2SO_4. The solutions used in the experiments were prepared with ultrapure water (Milli-Q 18.2 MΩ cm, Millipore System Inc.).

Electrochemical measurements were performed at room temperature using an AUTOLAB PGSTAT 302 N electrochemical workstation (Metrohm, Holland). A conventional three-electrode cell was employed, which involved a glassy carbon working electrode with a diameter of 2 mm, a platinum wire counter electrode, and a saturated silver/silver chloride reference electrode. All the potentials reported in this paper were obtained with respect to the reference electrode. All spectra were measured in PB buffer (0.1 M phosphate, pH 7.0) containing 0.1 M KCl and 2.5 mM $Fe(CN)_6^{3-/4-}$ as a redox couple. All experiments were performed at least three times to ensure the consistency of the response trend. In this study, a S4800 type scanning electron microscope (Hitachi, Japan) and a C1000 thermal PCR cycler (Bio-Rad, America) were also used.

Table 1
Base sequences of oligonucleotides used in this work.

Name	Base sequence
Oligo 1 (double labelled stem-loop probe)	5′-HS-C6-GCG AGG TTC CGT GGC TGC TGA TGA CTT GGT CCT CGC-biotin'
Oligo 2 (complementary target)	5′-ACC AAG TCA TCA GCA GCC ACG GAA-3′
Oligo 3 (single mismatch)	5′-ACC AAG TAA TCA GCA GCC ACG GAA-3′
Oligo 4 (non-complementary)	5′-GTT CGA CTG CTG ATG ATT GTA AGG-3′
Oligo 5 (upstream primer)	5′-AGA CTG GAG ACA ACC AAG AGA AG-3′
Oligo 6 (downstream primer)	5′-TTT CTT CCC TCA CAT GGC TAC C-3′

2.2. Fabrication of electrochemical DNA sensor

The GCE was treated with piranha solution (H_2SO_4:H_2O_2 = 7:3) and then rinsed with ultrapure water. Then, the GCE was polished to form a mirror sequentially with 0.3 and 0.05 μm alumina powder, followed by ultrasonic cleaning with ethanol and ultrapure water for 3 min each. The cleaned electrode was electrochemically pretreated in 0.5 M H_2SO_4 by potential scanning between −0.2 V and 1.6 V (vs Ag/AgCl) until a cyclic voltammogram (CV) characteristic of a clean electrode was obtained. Finally, the electrode was rinsed with ultrapure water and dried in air.

The pretreated electrode was immersed into a 0.1 mg Platinum nanoparticle ensemble-on-graphene hybrid nanosheet: One-pot, rapid synthesis, and used as new electrode material for electrochemical sensing mL^{-1} graphene oxide dispersion, and electrodeposited for 50 s with a control potential of −1.2 V (Qianfang Xia, Yang, & Li, 2012). The electrode was then removed from the dispersion, rinsed with ultrapure water, and dried. After that, the electrode was immersed into 0.1 mM $HAuCl_4$ solution, and electrodeposited for 50 s with a control potential of −0.25 V. The electrode was then removed from the dispersion, rinsed with ultrapure water, and dried. The above electrodeposition operation was performed in a cyclic manner by electrodepositing alternate monolayers of graphene and AuNPs to achieve a multilayer G–Au nanocomposite modified electrode after 3 cycles. After that, the electrode was electrodeposited for a further 500 s to form a compact layer of gold on the modified electrode surface, resulting in the formation of the graphene–gold nanocomposite/gold film electrode.

The immobilisation of the stem-loop probe was carried out by dropping a 4 μL stem-loop probe solution (1 μM) onto the surface of the G–Au nanocomposite/gold film electrode, kept at 4 °C overnight (Gang Liu et al., 2008). After that, the electrode was thoroughly rinsed with PBS buffer to remove any nonbonding materials. Then, 10 μL of PBS buffer containing 10 mM MCH was dropped onto the electrode surface for 30 min to block any remaining bare regions. Subsequently, the electrode was rinsed thoroughly with a copious amount of PBS buffer to remove the unattached MCH.

2.3. Hybridization and electrochemical measurement of the biosensor

The hybridization processes were performed by dropping 4 μL of a complementary target (Oligo 2), a single mismatch oligonucleotide (Oligo 3), or a non-complementary oligonucleotide (Oligo 4), onto the modified electrode surface, respectively, and the electrode maintained at 37 °C for 30 min. After hybridization, the electrode was rinsed with PBS buffer to remove any non-hybridized target DNA.

Cyclic voltammetry (CV) and electrochemical impedance spectroscopy (EIS) were applied to characterise the stepwise modification of the electrode surface. The specific hybridization process was monitored via differential pulse voltammetry (DPV). The scan rate in CV was 100 mV s^{-1} and the potential ranged from +0.6 V to −0.2 V. The EIS results were collected in the frequency range from 0.1 to 10^5 Hz with the amplitude of 0.01 V. The DPV from −0.2 to +0.6 V was carried out (0.005 V step potential, modulation amplitude 0.025 V, modulation time 0.05 s, interval time 0.5 s).

2.4. Detection of peanut allergen Ara h1 gene in peanut milk beverage

In order to test the real applicability of our new electrochemical DNA sensor, we applied it to the detection of the peanut allergen, the Ara h1 gene. The sample we used for detection was a peanut milk beverage (Yinlu, Xiamen), purchased from a nearby supermarket. The SDS-based method was used for extracting DNA from the peanut milk beverage (Pirondini et al., 2010). After the DNA was extracted, we used PCR amplification to amplify the extracted DNA. 7.5% PAGE gel electrophoresis was applied to identify the Ara h1 gene in the PCR products. We chose the 125-bp region in the Ara h1 gene (GenBank No. AF432231) (Kunmei Ji, Wang, Liu, & Liu, 2010). The 125-bp region was the target segment by PCR amplification. The loop sequence of the probe (Oligo 1) used in this study is the conserved sequence of the 125-bp region. The sequences of the upstream primer and the downstream primer are shown in Table 1. The amplification protocol was as follows, 10 min at 95 °C followed by 30 cycles at 95 °C for 30 s, 60 °C for 40 s, and 72 °C for 60 s. The reaction system was further incubated for 10 min at 72 °C to extend any incomplete products. After confirming the Ara h1 gene was extracted from peanut milk beverage, the recovery experiment was performed. A series of extracted DNA was prepared by adding target DNA at different concentrations. Then, the prepared DNA biosensor was used to detect the target DNA in these mixed samples.

3. Results and discussion

3.1. Schematic procedure of sensor fabrication

The stem-loop probe, dually labelled with 5′-SH and 3′-biotin, has six complementary bases at its 5′ and 3′ ends (five of them are G–C pairs), so that the DNA strand is closed by the thermostable G–C pairs to form a stem-loop. The stepwise fabrication process of the DNA biosensor is shown in Scheme 1. The sensor was constructed by cyclically electrodepositing alternate monolayers of graphene and AuNPs on the GCE surface to form a multilayer graphene–gold nanocomposite. A further layer of gold was electrodeposited on the surface of the multilayer graphene–gold nanocomposite. This enabled fixing of the stem-loop probe, creating a self-assembled monolayer of the immobilized stem-loop probe at the bioelectronic interface.

After this electrochemical deposition, the obtained electrodes were the gold film/graphene–gold nanocomposite/GCE. Through facile gold-thiol affinity, the probe was effectively assembled on the surface of the gold film/graphene–gold nanocomposite/GCE. Next, the electrode surface was blocked with MCH to decrease any non-specific adsorption of undesirable material to the modified electrode surface, which may reduce sensitivity of the DNA sensor. MCH/Probe/gold film/graphene–gold nanocomposite/GCE was then obtained. In the absence of the target DNA, the immobilised stem-loop probe was in the "closed" state, with the biotin unit located at the 3′ end in proximity to the electrode surface. Then the added target DNA was hybridized with the stem-loop probe, resulting in a conformational change of the probe. The stem-loop probe was kept in the "open" state for formation of the thermodynamically stable, rigid target probe duplex. Next, biotin was detached from the electrode surface. Electron-transfer efficiency was altered in the hybridization process, allowing the electrochemical signal to be detected for quantitative assay. This novel biosensor showed a good linear relationship between the current value and the logarithm of the target DNA concentration, as well as a low detection limit. Furthermore, the biosensor displayed improved mismatch discrimination between complementary targets, single-base mismatch and noncomplementary sequences.

3.2. Characterisation of the graphene–gold nanocomposite on the electrode surface

When the GCE was immersed into the 0.1 mg mL^{-1} graphene oxide dispersion, the surface of the GCE was covered completely

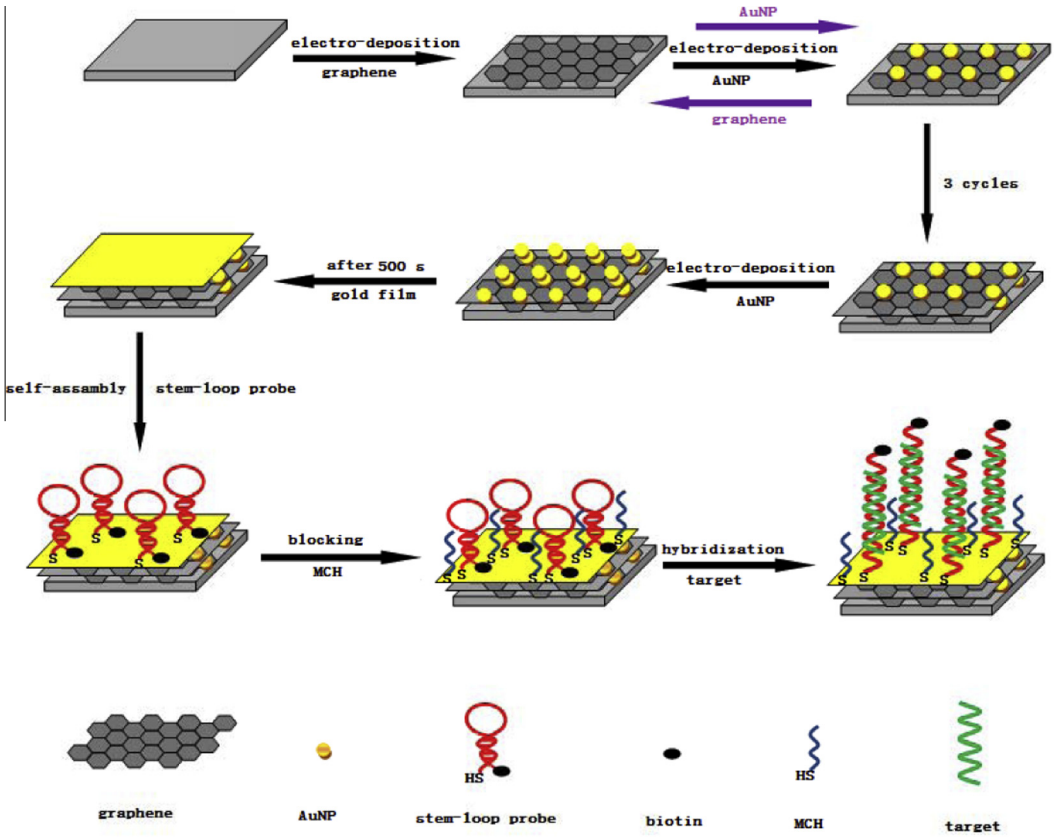

Scheme 1. Schematic illustration of the fabrication of the electrochemical stem-loop DNA biosensor.

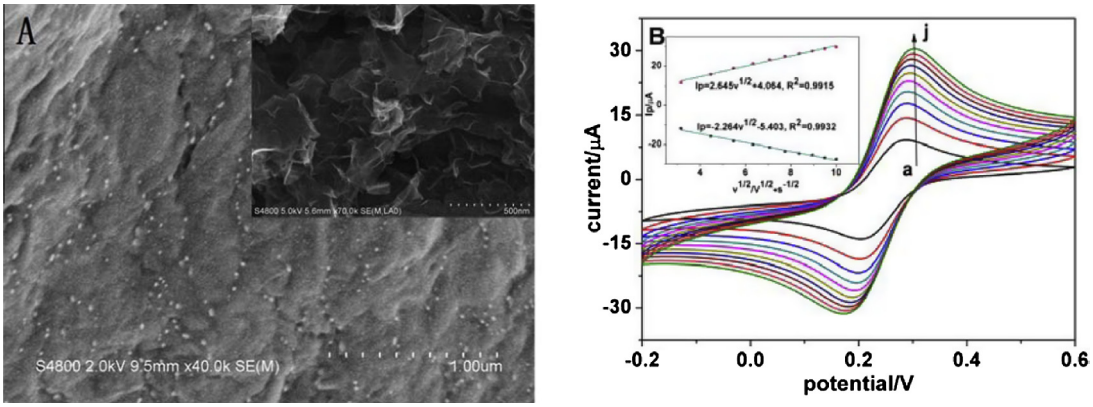

Fig. 1. (A) SEM image of a monolayer of the graphene–gold nanocomposite. (A) inset: SEM image of a monolayer of graphene. (B) Cyclic voltammograms of the G–Au composite/GCE at different scan rates of 10, 20, 30, 40, 50, 60, 70, 80, 90, 100 mV s^{-1} (a → j). (B) Inset: a plot of the linear regression of peak current (Ip) vs. square root of the scan rate ($v^{1/2}$).

by a single layer of graphene sheet after electrodeposition. As shown in the Fig. 1A inset, the graphene had a crumpled and wrinkled flake-like structure, which can increase the electrode effective surface. When the concentration of the $HAuCl_4$ solution was 0.1 mM, the surface of the graphene was covered uniformly by a single layer of AuNPs after electrodeposition to maintain good conductivity. As shown in Fig. 1A, the AuNPs were basically the same size, with diameters of about 10 nm. The electrodeposited AuNPs were spherical and uniformly dispersed between the graphene sheet layers. The cyclic electrodeposition methods are superior to the traditional dispensing method for preparing multilayer graphene–gold nanocomposite. While the prepared composite by the former is more uniform and does not easily fall from the electrode surface, the former is also more controllable and convenient.

We also investigated the influence of scan rate on the multilayer G–Au composite. As shown in Fig. 1B, an increase in the scan rate causes the peak current to increase. The linear relationship between the peak current (Ip/μA) and the square root of the scan rate ($v^{1/2}/V^{1/2} \cdot s^{-1/2}$) is shown in Fig. 1B inset. The regression equations, $Ip = 2.645v^{1/2} + 4.065$ ($R^2 = 0.9915$) and $Ip = -2.264v^{1/2} - 5.403$ ($R^2 = 0.9932$) indicate that the electrochemical reaction on the electrode surface is a reversible electrochemical process that is influenced by diffusion control (Li, Du, Yang, Liu, & Lu, 2012).

3.3. Electrochemical characterisation of the modified electrode

As shown in Fig. 2A and C, compared with the bare GCE (curve a), the peak current of the graphene/GCE (curve b), the graphene–gold nanocomposite/GCE (curve c), and the gold film/graphene–gold nanocomposite/GCE (curve d) increased gradually, while the peak-to-peak separation and impedance decreased d. Due to the good conductivity and large surface area of graphene for catalysing the redox reaction, the impedance of the GCE decreased significantly and peak current increased when the GCE was modified by graphene. Inserting highly conductive AuNPs between graphene sheets improved conductivity and electro-catalytic activity of the modified electrode. Therefore, impedance of the graphene–gold nanocomposite/GCE decreased further, and its peak current increased. Similarly, the impedance of the gold film/graphene–gold nanocomposite/GCE also decreased, while the peak current increased.

As shown in Fig. 2B and D, when the stem loop probes were assembled on the gold film/graphene–gold nanocomposite/GCE surface, the peak current decreased and the impedance increased (curve e). This indicates that the probes were immobilised successfully on the modified electrode surface. Since the stem loop probe occupied a large area on the modified electrode surface, the electrode could not efficiently exchange electrons with the solution. This reduced the electron-transfer efficiency of the electrode. After immobilisation of MCH, the peak current further decreased, while the impedance increased (curve f). After hybridization with the complementary target DNA, the stem-loop structure of the probe opened, enabling formation of the target-probe duplex. This directed the attached biotin group away from the electrode surface.

An earlier study shows that adding the complementary target DNA to the sensor causes the conductivity of the sensor to increase (Wang, He, Wang, & Ni, 2010). However, our study showed that the peak current decreased and the impedance increased after hybridization with the target nucleic acid (curve g). In fact, electron transfer efficiency can be affected by several factors. For example, biotin can decrease electron transfer efficiency with electrostatic repulsion of biotin's negative charge. Changing the probe's conformation can increase electron transfer efficiency due to a decrease in the space steric hindrance. Hybridization of the target can decrease electron transfer efficiency due to a decrease of the effective area on the electrode surface. Hybridization opens the stem-loop structures and allows target-probe duplex to form. After hybridization, the increased negative charges on the electrode surface repels negatively charged Fe(CN)63-/4-anions and further reduces the peak current. We found that the electron transfer efficiency decreases with the integration of all factors.

3.4. Quantificational detection of target DNA

To investigate the sensitivity of the prepared electrochemical DNA biosensor, we hybridized the sensor with different concentrations of targets. Then we measured the DPV current value as a response signal in 0.1 M PB (pH 7.0), containing 2.5 mM $Fe(CN)_6^{3-/4-}$ and 0.1 M KCl. The DPV signals obtained for different target concentrations are shown in Fig. 3. It is evident that in the series of target solutions with concentrations from 0.1 fM to 0.1 pM, the target concentration increased as the current signals decreased. The inset of Fig. 3 shows the tendency chart of the ΔI ($\Delta I = I_{\text{after hybridization}} - I_{\text{before hybridization}}$) as a function of the

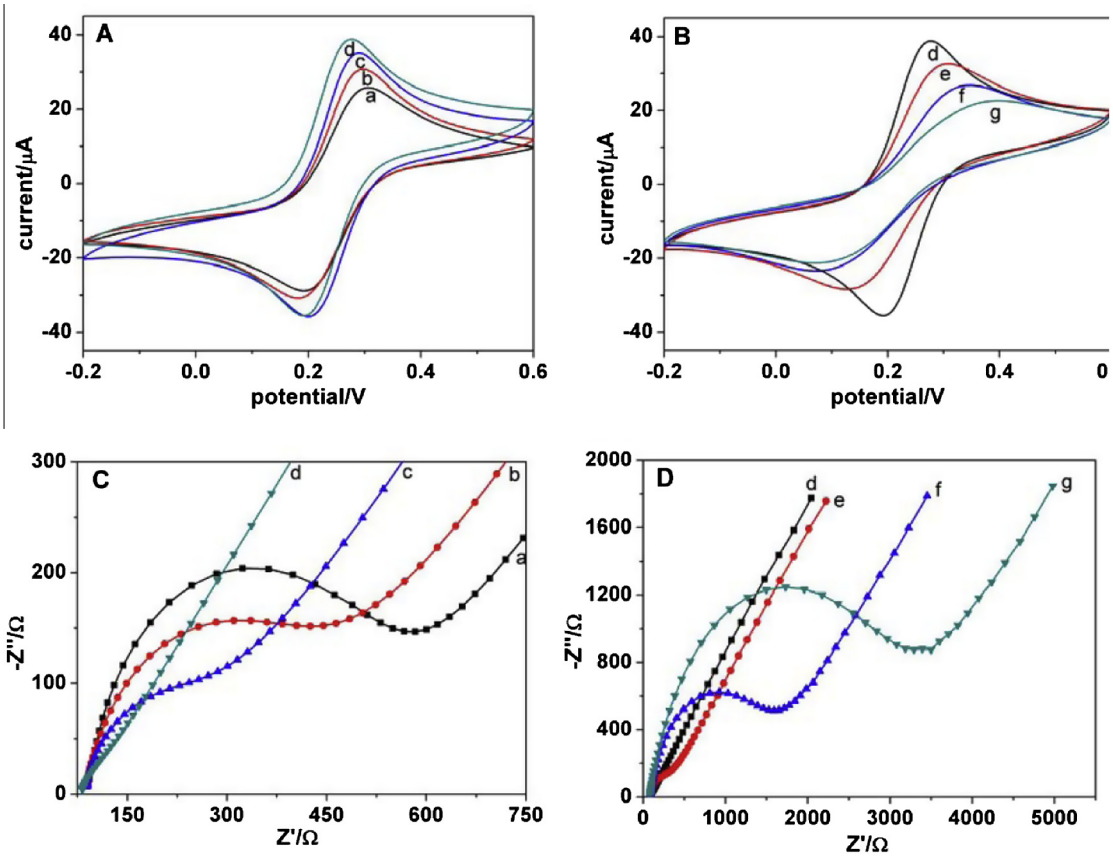

Fig. 2. Cyclic voltammograms (A and B) and Impedance spectra (C and D) of Bare GCE (a), graphene/GCE (b), graphene–gold nanoparticles/GCE (c), gold film/graphene–gold nanoparticles/GCE (d), hairpin probe/gold film/graphene–gold nanoparticles/GCE (e), MCH/hairpin probe/gold film/graphene–gold nanoparticles/GCE (f), target-probe duplex/MCH/gold film/graphene–gold nanoparticles/GCE (g) in 2.5 mM $Fe(CN)_6^{3-/4-}$ containing 0.1 M KCl.

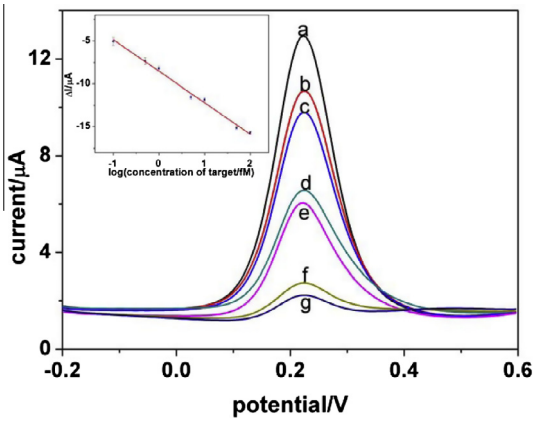

Fig. 3. Differential pulse voltammograms (DPVs) signals of the MCH/probe/gold film/G–Au composite/GCE after hybridization with complementary target DNA at a series of concentrations (from a to g: 0.1, 0.5, 1, 5, 10, 50 and 100 fM) in 2.5 mM $Fe(CN)_6^{3-/4-}$ containing 0.1 M KCl . Inset: Linear regression of ΔI (before and after hybridization) vs. the logarithm of target concentration (0.1–100 fM). Error bars relative standard deviation of three replicative tests.

target concentration, with a linear relationship between ΔI and the logarithm of the complementary target concentration. This is expressed in a regression equation, $\Delta I = -3.67358\log C - 8.53827$ and a correlation factor of 0.99198. The detection limit was 0.041 fM, as calculated according to the rule of three times the standard deviation over the background signal.

3.5. Selectivity of the DNA biosensor

We also examined the selectivity of the DNA biosensor was investigated, and the results are shown in Fig. 4. The prepared sensor was hybridized with various DNA sequences (complementary oligonucleotides, one base mismatch oligonucleotides and non-complementary oligonucleotides). Next, the DPV current value was measured. As shown in Fig. 4, compared with the immobilisation probe and MCH (curve a), the current value obtained after hybridization with the non-complementary oligonucleotides (curve b) was nearly identical, with a slight change in peak position. The current value after hybridization with the one-base mismatch oligonucleotides (curve c) decreased slightly. However, after hybridization with the complementary oligonucleotides (curve d), the current decreased markedly. This indicates that the immobilised stem-loop probes reacted only slightly with the one base mismatch and non-complementary oligonucleotides, and that complete hybridization was not accomplished due to the base mismatch. Therefore, the prepared DNA biosensor shows excellent selectivity for detection of target DNA sequences. This indicates that this DNA biosensor is particularly effective at discriminating between non-complementary or single-base mismatch oligonucleotides and complementary oligonucleotides.

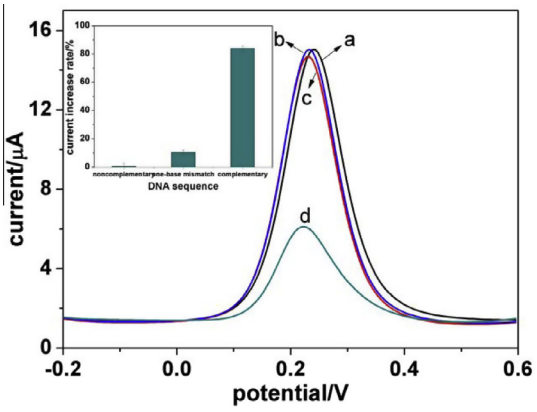

Fig. 4. Differential pulse voltammograms (DPVs) signals for MCH/probe/gold film/G–Au composite/GCE (a), and after hybridization at 37 °C with 10^{-14} M non-complementary (b), one-base mismatch (c) and the complementary DNA (d) in 2.5 mM $Fe(CN)_6^{3-/4-}$ containing 0.1 M KCl. Inset: The bar graphs of DPV signals when the hairpin probe hybridized with different DNA sequences. Error bars relative standard deviation of three replicative tests.

3.6. Optimisation of experimental conditions

There was a large Van der Waals force between the graphene sheets, making it easy for the graphene sheets easy to accumulate and aggregate. Therefore, the electron transfer efficiency decreased and impedance increased. This problem limited application of graphene sheets. Therefore, we inserted gold nanoparticles between the graphene sheets to prevent aggregation and improve electron conductivity. When graphene was prepared by electrodeposition; the electrodeposition time should be controlled to form monolayer graphene sheets. As shown in Fig. s1A, the monolayer graphene sheet formed gradually, so that the current increased gradually prior to 50 s. After 50 s, the current decreased. This indicates that the graphene sheets may have accumulated on the electrode surface, decreasing electron transfer efficiency. Thus, we chose 50 s as the optimal time for graphene electrodeposition in this study.

To get the optimal electrical conductivity of the multilayer graphene–gold nanocomposite, we also counted nanocomposite layers. As shown in Fig. s1B, the current of the modified electrode increased with more nanocomposite layers. However, beyond the third layer, the current decreased. Although the current value of every layer nanocomposite increased, this was minimal. Due to thickening of the electrode surface membrane, the electron transfer efficiency decreased. To save electrode modification time, we selected three layers as the optimal number of the multilayer graphene–gold nanocomposite.

We also analysed the hybridization time and temperature between the probe and the target with electrochemical impedance spectroscopy. We determined the best hybridization time using the probe (10^{-6} M) in hybridizations with target DNA (10^{-13} M) for different times. Fig. s2 A displays the effect of hybridization time on charge transfer resistance. From 0 to 75 min, the Ret value increased gradually, with the signal increasingly only slightly or not at all during longer times. Therefore, we chose 30 min for the hybridization time as a time-saving consideration. Hybridization temperature is very important. Hybridization should be carried out at a suitable temperature to ensure successful detection of Ara h1 gene using the proposed strategy. Many studies have shown that the optimal temperature for hybridization is 25 °C below the melting temperature (Tm) (Tang et al., 2009). In our study, the probe Tm was 74.61 °C and the theoretical optimal hybridization temperature was under 50 °C. Fig. s2 B shows the effects of hybridization temperature (15–55 °C) on the impedance response of the sensor. The maximum Ret was observed at around 35–40 °C. When the hybridization temperature increased continuously, the peak current showed no obvious change. Therefore, 37 °C was used for hybridization of the probe and the target in subsequent experiments.

3.7. Reproducibility and stability of the DNA biosensor

To demonstrate reproducibility of this electrochemical assay, we immersed the hybridized electrode in 50 mM NaOH for 1 min, washed it with PBS, and then rehybridized with the target sequence (Wang Qingxiang, Xiaoqiang, & Wen, 2011). After five

Table 2
Recovery experiment results of Ara h1 gene from peanut milk beverage by the biosensor.

The concentration of the added target (fM)	ΔI (μA)	The detected concentration of target (fM)	Recovery (%)	RSD (%)
1	−8.3124	0.868	86.8	2.9
10	−12.0379	8.967	89.67	2.3
50	−14.9381	55.223	110.4	6.7
100	−15.8212	96.054	97.05	4.1

rounds of regeneration, we found that the DNA biosensor had retained its 85% original value. This illustrates well the reproducible characteristic of the prepared DNA biosensor.

We also evaluated stability of the DNA biosensor over a 21-day period. After refrigeration of the sensor hybridized with target DNA at 4 °C for 21 days, the DPV peak current of the sensor retained 82% of its initial response. This indicates good stability in the developed DNA biosensor.

3.8. Detection of the peanut allergen Ara h1 in peanut milk beverage

Ara h1 is a 7S vicilin-like globulin also known as conarachin. Essentially, 12–16% of total peanut proteins are constituted by Ara h1. This affects 35–95% of peanut allergic patients in different populations, highlighting the importance of developing a sensor capable of detecting Ara h1 in foods. Commercial production processes involve heat treatment, which often denatures Ara h1 proteins. This alters the protein tertiary structure and hinders protein detection. However, since DNA remains intact for a longer time under heat and pressure processing, it can provide the basis of a robust assay to detect Ara h1 residues in foods.

This PCR study (Fig. s3) confirmed the successful extraction of the Ara h1 gene from peanut milk beverage using the 125 bp sequence as the amplified target and a 20 bp sequence as the primer dimer. Next, the extracted genomic DNA from peanut milk beverage was used in the recovery experiment. Analytical results were shown in Table 2. Results show recovery of the Ara h1 gene (between 86.8% and 110.4%) from the peanut milk beverage and relative standard deviation values (between 2.3% and 6.7%) are acceptable.

4. Conclusions

In this study, we demonstrated a new electrochemical DNA biosensor that combines a multilayer graphene–gold nanocomposite and an immobilised stem-loop probe, dually labelled with 5′-SH and 3′-biotin. The DNA biosensor showed high sensitivity, confirmed by the detection limit, which reached 0.041 fM. The DNA biosensors displayed excellent selectivity for detection of target DNA sequences. It was also effective for determining peanut DNA extracts. Recovery of the Ara h1 gene from the peanut milk beverage tested ranged from 86.8% and 110.4%, while relative standard deviation values ranged between 2.3% and 6.7%. Therefore, the proposed electrochemical assay with this new electrochemical DNA biosensor shows promise for application in the clinical diagnosis of peanut allergens and in food safety control.

Acknowledgements

This work has been supported by National Research Program (No. 2011BAK10B03), "973" National Basic Research Program of China (No. 2012CB720804), Commonweal Project of the Ministry of Agriculture (No. 201203069-1), the Program for New Century Excellent Talents in Jiangnan University, Qinglan Project, Synergetic Innovation Center of Food Safety and quality control, and the Priority Academic Program Development of Jiangsu Higher Education Institutions.

Appendix A. Supplementary data

Supplementary data associated with this article can be found, in the online version, at http://dx.doi.org/10.1016/j.foodchem.2014.09.042.

References

Barr Fritcher, E. G., Brankley, S. M., Kipp, B. R., Voss, J. S., Campion, M. B., Morrison, L. E., et al. (2008). A comparison of conventional cytology, DNA ploidy analysis, and fluorescence in situ hybridization for the detection of dysplasia and adenocarcinoma in patients with Barrett's esophagus. *Human Pathology, 39*(8), 1128–1135.

Bockisch, B., Thomas, G., Edzard, Spillner, & Reinhard, Bredehorst (2005). Immobilized stem-loop structured probes as conformational switches for enzymatic detection of microbial 16S rRNA. *Nucleic Acids Research, 33*(11), e101.

Chen, J., Zhang, J., Yang, H., Fu, F., & Chen, G. (2010). A strategy for development of electrochemical DNA biosensor based on site-specific DNA cleavage of restriction endonuclease. *Biosensors & Bioelectronics, 26*(1), 144–148.

Ehsan Salamifar, S., & Lai, R. Y. (2014). Fabrication of electrochemical DNA sensors on gold-modified recessed platinum nanoelectrodes. *Analytical Chemistry, 86*(6), 2849–2852.

Elias, D. C., Nair, R. R., Mohiuddin, T. M. G., Morozov, S. V., Blake, P., Halsall, M. P., et al. (2009). Control of graphene's properties by reversible hydrogenation: Evidence for graphane. *Science, 323*(5914), 610–613.

Espy, M. J., Uhl, J. R., Sloan, L. M., Rosenblatt, J. E., Cockerill Iii, F. R., & Smith, T. F. (2002). Detection of vaccinia virus, herpes simplex virus, varicella-zoster virus, and bacillus anthracis DNA by LightCycler polymerase chain reaction after autoclaving: Implications for biosafety of bioterrorism agents. *Mayo Clinic Proceedings, 77*(7), 624–628.

Fan, H., Xing, R., Xu, Y., Chen, M., Wang, Q., He, P., et al. (2010). A competitor-switched electrochemical sensor for detection of DNA. *Chinese Journal of Chemistry, 28*(10), 1978–1982.

Goel, G., Kumar, A., Puniya, A. K., Chen, W., & Singh, K. (2005). Molecular beacon: A multitask probe. *Journal of Applied Microbiology, 99*(3), 435–442.

Gu, Zhiguo, Shuping, Yang, Li, Zaijun, Sun, Xiulan, Wang, Guangli, Fang, Yinjun, et al. (2011). An ultrasensitive electrochemical biosensor for glucose using CdTe–CdS core–shell quantum dot as ultrafast electron transfer relay between graphene–gold nanocomposite and gold nanoparticle. *Electrochimica Acta, 56*(25), 9162–9167.

Guo, S., Wen, D., Zhai, Y., Dong, S., & Wang, E. (2010). Platinum nanoparticle ensemble-on-graphene hybrid nanosheet: One-pot, rapid synthesis, and used as new electrode material for electrochemical sensing. *ACS Nano, 4*(7), 3959–3968.

Huang, Daming, Liu, He, Zhang, Bo, Jiao, Kui, & Xun, Fu (2009). Highly sensitive electrochemical detection of sequence-specific DNA of 35S promoter of cauliflower mosaic virus gene using CdSe quantum dots and gold nanoparticles. *Microchimica Acta, 165*(1–2), 243–248.

Kjallman, T. H. M., Peng, H., Soeller, C., & Travas-Sejdic, J. (2010). A CdTe nanoparticle-modified hairpin probe for direct and sensitive electrochemical detection of DNA. *Analyst, 135*(3), 488–494.

Kunmei Ji, J. C., Wang, Haiyan, Liu, Xiaoyu, & Liu, Zhigang (2010). Development of a TaqMan real-time quantitative PCR for detection of peanut allergen Ara h1 DNA residue in foods. *Food Research and Development, 31*(12), 188–193.

Li, X., Cai, W., An, J., Kim, S., Nah, J., Yang, D., et al. (2009). Large-area synthesis of high-quality and uniform graphene films on copper foils. *Science, 324*(5932), 1312–1314.

Li, Y., Du, J., Yang, J., Liu, D., & Lu, X. (2012). Electrocatalytic detection of dopamine in the presence of ascorbic acid and uric acid using single-walled carbon nanotubes modified electrode. *Colloids and Surfaces B: Biointerfaces, 97*, 32–36.

Lin, L., Lin, X., Chen, J., Chen, W., He, M., & Chen, Y. (2009). Electrochemical biosensor for detection of BCR/ABL fusion gene based on hairpin locked nucleic acids probe. *Electrochemistry Communications, 11*(8), 1650–1653.

Lin, L., Liu, Q., Wang, L., Liu, A., Weng, S., Lei, Y., et al. (2011). Enzyme-amplified electrochemical biosensor for detection of PML–RARα fusion gene based on hairpin LNA probe. *Biosensors & Bioelectronics, 28*(1), 277–283.

Liu, Gang, Wan, Y., Gau, Vincent, Zhang, Jiong, Wang, Lihua, Song, Shiping, et al. (2008). An enzyme-based E-DNA sensor for sequence-specific detection of femtomolar DNA targets. *Journal of the American Chemical Society, 130*(21), 6820–6825.

Liu, Zhongyuan, Zhang, W., Zhu, Shuyun, Zhang, Ling, Lianzhe, Hu, Parveen, Saima, et al. (2011). Ultrasensitive signal-on DNA biosensor based on nicking endonuclease assisted electrochemistry signal amplification. *Biosensors & Bioelectronics, 29*(1), 215–218.

Mekata, T., Sudhakaran, R., Kono, T., U-taynapun, K., Supamattaya, K., Suzuki, Y., et al. (2009). Real-time reverse transcription loop-mediated isothermal amplification for rapid detection of yellow head virus in shrimp. *Journal of Virological Methods, 162*(1–2), 81–87.

Park, S., & Ruoff, R. S. (2009). Chemical methods for the production of graphenes. *Nature Nanotechnology, 4*(4), 217–224.

Paunovic, M. (2007). *Electrochemical deposition*. Wiley Online Library.

Pirondini, A., Bonas, U., Maestri, E., Visioli, G., Marmiroli, M., & Marmiroli, N. (2010). Yield and amplificability of different DNA extraction procedures for traceability in the dairy food chain. *Food Control, 21*(5), 663–668.

Pumera, M., Sanchez, S., Ichinose, I., & Tang, J. (2007). Electrochemical nanobiosensors. *Sensors and Actuators B: Chemical, 123*(2), 1195–1205.

Qianfang Xia, Y. H., Yang, Xue, & Li, Zaijun (2012). Preparation and its application of novel graphene/gold/functional conducting polymer/hydrogen peroxide biosensor. *Acta Chimica Sinica, 70*(11), 1315–1321.

Rai, V., Nyine, Y. T., Hapuarachchi, H. C., Yap, H. M., Ng, L. C., & Toh, C.-S. (2012). Electrochemically amplified molecular beacon biosensor for ultrasensitive DNA sequence-specific detection of Legionella sp. *Biosensors & Bioelectronics, 32*(1), 133–140.

Summerer, D., & Marx, A. (2002). A molecular beacon for quantitative monitoring of the DNA polymerase reaction in real-time. *Angewandte Chemie International Edition, 41*(19), 3620–3622.

Tang, L., Zeng, G., Shen, G., Li, Y., Liu, C., Li, Z., et al. (2009). Sensitive detection of *lip* genes by electrochemical DNA sensor and its application in polymerase chain reaction amplicons from *Phanerochaete chrysosporium*. *Biosensors & Bioelectronics, 24*(5), 1474–1479.

Wang, Y., He, X., Wang, K., & Ni, X. (2010). A sensitive ligase-based ATP electrochemical assay using molecular beacon-like DNA. *Biosensors & Bioelectronics, 25*(9), 2101–2106.

Wang Qingxiang, Z. B., Xiaoqiang, Lin., & Wen, Weng (2011). Hybridization biosensor based on the covalent immobilization of probe DNA on chitosan–mutiwalled carbon nanotubes nanocomposite by using glutaraldehyde as an arm linker. *Sensors and Actuators B: Chemical, 156*(2), 599–605.

Wang, J., Zhang, S., & Zhang, Y. (2010). Fabrication of chronocoulometric DNA sensor based on gold nanoparticles/poly(l-lysine) modified glassy carbon electrode. *Analytical Biochemistry, 396*(2), 304–309.

Wenjing Hong, H. B., Yuxi, Xu, Yao, Zhiyi, Zhongze, Gu, & Shi, Gaoquan (2010). Preparation of gold nanoparticle/graphene composites with controlled weight contents and their application in biosensors. *The Journal of Physical Chemistry C, 114*(4), 1822–1826.

Xu, C., Wang, X., & Zhu, J. (2008). Graphene−metal particle nanocomposites. *The Journal of Physical Chemistry C, 112*(50), 19841–19845.

Yan, X., Cui, X., & Li, L. S. (2010). Synthesis of large, stable colloidal graphene quantum dots with tunable size. *Journal of the American Chemical Society, 132*(17), 5944–5945.

Yin, H., Zhou, Y., Zhang, H., Meng, X., & Ai, S. (2012). Electrochemical determination of microRNA-21 based on graphene, LNA integrated molecular beacon, AuNPs and biotin multifunctional bio bar codes and enzymatic assay system. *Biosensors & Bioelectronics, 33*(1), 247–253.

Yu, Z.-G., & Lai, R. Y. (2012). A reagentless and reusable electrochemical DNA sensor based on target hybridization-induced stem-loop probe formation. *Chemical Communications, 48*(85), 10523–10525.

Zheng, M., Zhang, L., Li, G., & Shen, W. (2002). Fabrication and optical properties of large-scale uniform zinc oxide nanowire arrays by one-step electrochemical deposition technique. *Chemical Physics Letters, 363*(1), 123–128.

Zhong, Z., Wu, W., Wang, D., Wang, D., Shan, J., Qing, Y., et al. (2010). Nanogold-enwrapped graphene nanocomposites as trace labels for sensitivity enhancement of electrochemical immunosensors in clinical immunoassays: Carcinoembryonic antigen as a model. *Biosensors & Bioelectronics, 25*(10), 2379–2383.

Zuccarelli, G., Alechine, E., Caputo, M., Bobillo, C., Corach, D., & Sala, A. (2011). Rapid screening for Native American mitochondrial and Y-chromosome haplogroups detection in routine DNA analysis. *Forensic Science International: Genetics, 5*(2), 105–108.